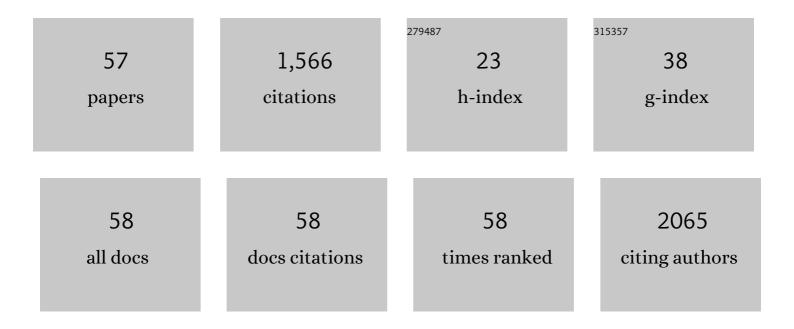
## You Wang

## List of Publications by Year in descending order

Source: https://exaly.com/author-pdf/3486072/publications.pdf Version: 2024-02-01



#	Article	IF	CITATIONS
1	The elemental 2D materials beyond graphene potentially used as hazardous gas sensors for environmental protection. Journal of Hazardous Materials, 2022, 423, 127148.	6.5	27
2	Synergically engineering defect and interlayer in SnS2 for enhanced room-temperature NO2 sensing. Journal of Hazardous Materials, 2022, 421, 126816.	6.5	36
3	N dopants triggered new active sites and fast charge transfer in MoS2 nanosheets for full Response-Recovery NO2 detection at room temperature. Applied Surface Science, 2022, 571, 151162.	3.1	20
4	Construction of Z-scheme heterojunction by coupling Bi2Sn2O7 and BiOBr with abundant oxygen vacancies: Enhanced photodegradation performance and mechanism insight. Journal of Colloid and Interface Science, 2022, 612, 550-561.	5.0	33
5	Bifunctional gas sensor based on Bi <sub>2</sub> S <sub>3</sub> /SnS <sub>2</sub> heterostructures with improved selectivity through visible light modulation. Journal of Materials Chemistry A, 2022, 10, 4306-4315.	5.2	46
6	A Comparison Study of the Friction and Wear Behavior of Nanostructured Al2O3-YSZ Composite Coatings With and Without Nano-MoS2. Journal of Thermal Spray Technology, 2022, 31, 415-428.	1.6	2
7	Boosting room-temperature NO2 detection via in-situ interfacial engineering on Ag2S/SnS2 heterostructures. Journal of Hazardous Materials, 2022, 434, 128782.	6.5	21
8	A Novel Nanostructured Mullite Feedstock for Environmental Barrier Coatings via Atmosphere Plasma Spraying. Crystals, 2022, 12, 726.	1.0	1
9	Boosted interfacial charge transfer in SnO <sub>2</sub> /SnSe <sub>2</sub> heterostructures: toward ultrasensitive room-temperature H <sub>2</sub> S detection. Inorganic Chemistry Frontiers, 2021, 8, 2068-2077.	3.0	23
10	Carbon-doping-induced energy-band modification and vacancies in SnS <sub>2</sub> nanosheets for room-temperature ppb-level NO <sub>2</sub> detection. Inorganic Chemistry Frontiers, 2021, 8, 5006-5015.	3.0	15
11	Engineering SnO <sub>2</sub> nanorods/ethylenediamine-modified graphene heterojunctions with selective adsorption and electronic structure modulation for ultrasensitive room-temperature NO <sub>2</sub> detection. Nanotechnology, 2021, 32, 155505.	1.3	14
12	Boosted charge transfer in dual Z-scheme BiVO4@ZnIn2S4/Bi2Sn2O7 heterojunctions: Towards superior photocatalytic properties for organic pollutant degradation. Chemosphere, 2021, 276, 130226.	4.2	49
13	Design of hierarchical SnSe <sub>2</sub> for efficient detection of trace NO <sub>2</sub> at room temperature. CrystEngComm, 2021, 23, 6045-6052.	1.3	13
14	Cell membrane camouflaged cerium oxide nanocubes for targeting enhanced tumor-selective therapy. Journal of Materials Chemistry B, 2021, 9, 9524-9532.	2.9	9
15	Preparation and study of cerium lanthanum zirconate fibres. Philosophical Magazine Letters, 2021, 101, 484-492.	0.5	0
16	Increased Active Sites and Charge Transfer in the SnS <sub>2</sub> /TiO <sub>2</sub> Heterostructure for Visible-Light-Assisted NO <sub>2</sub> Sensing. ACS Applied Materials & Interfaces, 2021, 13, 54152-54161.	4.0	32
17	Ce-Substituted Nanograin Na <sub>3</sub> Zr <sub>2</sub> Si <sub>2</sub> PO <sub>12</sub> Prepared by LF-FSP as Sodium-Ion Conductors. ACS Applied Materials & Interfaces, 2020, 12, 3502-3509.	4.0	29
18	Ultralow-intensity near infrared light synchronously activated collaborative chemo/photothermal/photodynamic therapy. Biomaterials Science, 2020, 8, 607-618.	2.6	22

YOU WANG

#	Article	IF	CITATIONS
19	Depth-Sensing Indentation Creep Behavior of Nanostructured Thermal Barrier Coatings from As-Synthesized t'-8YSZ Feedstocks. Nanomaterials, 2020, 10, 38.	1.9	3
20	Al2O3/TiO2-Ni-WC Composite Coatings Designed for Enhanced Wear Performance by Laser Cladding Under High-Frequency Micro-Vibration. Jom, 2020, 72, 4060-4068.	0.9	5
21	Photothermal Generation of Oxygen-Irrelevant Free Radicals with Simultaneous Suppression of Glutathione Synthesis for an Enhanced Photonic Thermodynamic Cancer Therapy. ACS Biomaterials Science and Engineering, 2020, 6, 6186-6194.	2.6	12
22	Microstructure and properties evolution of plasma sprayed Al2O3-ZrO2-TiO2 coatings during high temperature and thermal shock resistance. Materials at High Temperatures, 2020, 37, 256-267.	0.5	1
23	Microstructure and Properties of Al2O3–ZrO2–Y2O3 Composite Coatings Prepared by Plasma Spraying. Journal of Thermal Spray Technology, 2020, 29, 967-978.	1.6	14
24	Microstructural evolution and wear behaviors of NbC-reinforced Ti-based composite coating. International Journal of Advanced Manufacturing Technology, 2020, 107, 2397-2407.	1.5	15
25	2D/2D heterojunction of g–C <sub>3</sub> N <sub>4</sub> /SnS <sub>2</sub> : room-temperature sensing material for ultrasensitive and rapid-recoverable NO <sub>2</sub> detection. Nanotechnology, 2020, 31, 425502.	1.3	28
26	Synergy of charge pre-separation and direct Z-scheme bridge in BiVO4{0Â4Â0}/Ag6Si2O7 photocatalyst boosting organic pollutant degradation. Applied Surface Science, 2020, 513, 145832.	3.1	34
27	High temperature microstructure evolution and thermal shock resistance of plasma sprayed Al2O3-ZrO2-CeO2 coatings. Journal of Vacuum Science and Technology A: Vacuum, Surfaces and Films, 2020, 38, .	0.9	4
28	Dendrimerâ€Based, High‣uminescence Conjugated Microporous Polymer Films for Highly Sensitive and Selective Volatile Organic Compound Sensor Arrays. Advanced Functional Materials, 2020, 30, 1910275.	7.8	71
29	A cascade-reaction enabled synergistic cancer starvation/ROS-mediated/chemo-therapy with an enzyme modified Fe-based MOF. Biomaterials Science, 2019, 7, 3683-3692.	2.6	78
30	Electrophoretically Deposited <i>p</i> -Phenylene Diamine Reduced Graphene Oxide Ultrathin Film on LiNi <sub>0.5</sub> Mn <sub>1.5</sub> O <sub>4</sub> Cathode to Improve the Cycle Performance. ACS Applied Materials & Interfaces, 2019, 11, 35667-35674.	4.0	15
31	Effects of laser processing parameters on microstructure and mechanical properties of additively manufactured AlSi10Mg alloys reinforced by TiC. International Journal of Advanced Manufacturing Technology, 2019, 103, 3235-3246.	1.5	21
32	Enhancement of ultralow-intensity NIR light-triggered photodynamic therapy based on exo- and endogenous synergistic effects through combined glutathione-depletion chemotherapy. Nanoscale, 2019, 11, 13078-13088.	2.8	32
33	SnS <sub>2</sub> /SnS p–n heterojunctions with an accumulation layer for ultrasensitive room-temperature NO <sub>2</sub> detection. Nanoscale, 2019, 11, 13741-13749.	2.8	116
34	<p>Ultralow-intensity NIR light triggered on-demand drug release by employing highly emissive UCNP and photocleavable linker with low bond dissociation energy</p> . International Journal of Nanomedicine, 2019, Volume 14, 4017-4028.	3.3	6
35	Facile preparation of pyrenemethyl ester-based nanovalve on mesoporous silica coated upconversion nanoparticle for NIR light-triggered drug release with potential monitoring capability. Colloids and Surfaces A: Physicochemical and Engineering Aspects, 2019, 568, 436-444.	2.3	27
36	Decorating Ag <sub>3</sub> PO <sub>4</sub> nanodots on mesoporous silica-functionalized NaYF <sub>4</sub> Yb,Tm@NaLuF <sub>4</sub> for efficient sunlight-driven photocatalysis: synergy of broad spectrum absorption and pollutant adsorption-enrichment. Inorganic Chemistry Frontiers, 2019, 6, 3529-3538.	3.0	16

You Wang

#	Article	IF	CITATIONS
37	Hierarchical SnS <sub>2</sub> /SnO <sub>2</sub> nanoheterojunctions with increased active-sites and charge transfer for ultrasensitive NO <sub>2</sub> detection. Nanoscale, 2018, 10, 7210-7217.	2.8	136
38	Rapid recognition of volatile organic compounds with colorimetric sensor arrays for lung cancer screening. Analytical and Bioanalytical Chemistry, 2018, 410, 3671-3681.	1.9	41
39	Meltâ€mixing small diameter glass fiber and epoxy resin in internal mixer without solvent for strain gage substrate. Polymer Composites, 2018, 39, 1321-1330.	2.3	0
40	Highly sensitive and rapidly responding room-temperature NO2 gas sensors based on WO3 nanorods/sulfonated graphene nanocomposites. Nano Research, 2018, 11, 791-803.	5.8	98
41	Near-Infrared Light-Triggered Hydrophobic-to-Hydrophilic Switch Nanovalve for On-Demand Cancer Therapy. ACS Biomaterials Science and Engineering, 2018, 4, 3478-3486.	2.6	24
42	Effect of Nano-Si3N4 Additives and Plasma Treatment on the Dry Sliding Wear Behavior of Plasma Sprayed Al2O3-8YSZ Ceramic Coatings. Journal of Thermal Spray Technology, 2017, 26, 764-777.	1.6	9
43	Crystallographic and topographical evolutions of a cylinder patterned sapphire substrate etched with a sulfuric acid and phosphoric acid mixture: an SEM and AFM study. CrystEngComm, 2017, 19, 6383-6390.	1.3	6
44	Competitive-Binding Activated Supramolecular Nanovalves Based on β-Cyclodextrin Complexes. ChemistrySelect, 2017, 2, 5341-5347.	0.7	2
45	Fabrication of Mesoporousâ€Silicaâ€Coated Upconverting Nanoparticles with Ultrafast Photosensitizer Loading and 808 nm NIRâ€Lightâ€Triggering Capability for Photodynamic Therapy. Chemistry - an Asian Journal, 2017, 12, 2197-2201.	1.7	27
46	Thermal Evolution of Three Selected Preceramic POSSs Into Ceramic Materials. Journal of Inorganic and Organometallic Polymers and Materials, 2017, 27, 1292-1301.	1.9	0
47	Near-infrared light activated photodynamic therapy of THP-1 macrophages based on core-shell structured upconversion nanoparticles. Microporous and Mesoporous Materials, 2017, 239, 78-85.	2.2	21
48	Hedgehog Buckyball: A High-Symmetry Complete Polyhedral Oligomeric Silsesquioxane (POSS). Polymers, 2016, 8, 315.	2.0	4
49	pH-Responsive drug release and NIR-triggered singlet oxygen generation based on a multifunctional core–shell–shell structure. Physical Chemistry Chemical Physics, 2016, 18, 25497-25503.	1.3	35
50	Design and Synthesis of Core–Shell–Shell Upconversion Nanoparticles for NIR-Induced Drug Release, Photodynamic Therapy, and Cell Imaging. ACS Applied Materials & Interfaces, 2016, 8, 4416-4423.	4.0	103
51	Triple-doped KMnF3:Yb3+/Er3+/Tm3+ nanocubes: four-color upconversion emissions with strong red and near-infrared bands. Scientific Reports, 2015, 5, 17088.	1.6	18
52	Modification of a Phenolic Resin with Epoxy- and Methacrylate-Functionalized Silica Sols to Improve the Ablation Resistance of Their Glass Fiber-Reinforced Composites. Polymers, 2014, 6, 105-113.	2.0	16
53	Nanocomposite Lanthanum Zirconate Thermal Barrier Coating Deposited by Suspension Plasma Spray Process. Journal of Thermal Spray Technology, 2014, 23, 1030-1036.	1.6	34
54	Optimization of Processing Parameters for WC-11Co Cemented Carbide Doped with Nano-Crystalline CeO2. Journal of Materials Engineering and Performance, 2013, 22, 112-117.	1.2	8

You Wang

#	Article	IF	CITATIONS
55	One-dimensional hierarchical Bi2WO6 hollow tubes with porous walls: synthesis and photocatalytic property. CrystEngComm, 2013, 15, 4124.	1.3	51
56	Mechanical Properties and Thermal Shock Resistance of HVOF Sprayed NiCrAlY Coatings Without and With Nano Ceria. Journal of Thermal Spray Technology, 2012, 21, 818-824.	1.6	26
57	Facile measurement of polymer film thickness ranging from nanometer to micrometer scale using atomic force microscopy. Surface and Interface Analysis, 2011, 43, 1299-1303.	0.8	17